0945070132 – 1

Source Identification, Counterparts and Properties

STONKS alert

- Type of Alert: Low flux state,
- Long-term Variability $= 5.8$,
- No short-term Variability.

The long-term variability is the difference between the upper limit of the flux lowest value and the lower limit of the flux highest value.

The short-term variability is the result of a χ^2 test of the flux against a constant value.

XMM-Newton Science Archive

https://nxsa.esac.esa.int/nxsa-web/#search

Simbad

https://simbad.cds.unistra.fr/simbad/sim-id?Ident=%4016018930&Name=4FGL%20J0333.4-2705&submit=submit

The source is identified on Simbad as a Gamma-Ray Source: *4FGL J0333.4-2705*.

ESASky

https://sky.esa.int/esasky/?target=53.59466666666666%20-28.902777777777782&hips=DSS2+color&fov=1&projection=SIN&cooframe=J2000&sci=true&lang=fr

The source has multiple counterparts on ESASky:

- EPIC Stack (Soft X-ray),
- XMM Slew (Soft X-ray),
- eROSITA eRASS1 main (Soft X-ray),
- XMM-SUSS 6.2 (UV to Optical),
- Gaia DR3 (Optical),
- Euclid MER Q1 (Optical to Near-IR),
- AllWISE (Near-IR to Mid-IR).

Gaia DR3 gives the following useful data:

- Parallax: $P = 0.1954\ mas \rightarrow d \approx 5.11\ kpc$,
- Magnitude: $G = 19.7505$,
- $G_{BP} - G_{RP} = 0.8773$.

The source is faint and most likely Extragalactic.

Gaia DR3 also gives a probability of classification:

- Classprob Dsc Combmod Galaxy $= 0.0002$,
- Classprob Dsc Combmod Quasar $= 0.9957$,
- Classprob Dsc Combmod Star $= 0.0042$.

The probabilities tend to classify as a **quasar**.

There are 6 publications:

https://ui.adsabs.harvard.edu/abs/2022A%26A...660A..87B/abstract

https://ui.adsabs.harvard.edu/abs/2022ApJS..260...53A/abstract

https://ui.adsabs.harvard.edu/abs/2021ApJ...914...42B/abstract

https://ui.adsabs.harvard.edu/abs/2021MNRAS.505.5853G/abstract

https://ui.adsabs.harvard.edu/abs/2021ApJ...923...75K/abstract

https://ui.adsabs.harvard.edu/abs/2020ApJS..247...33A/abstract

3DNH-tool

http://astro.uni-tuebingen.de/nh3d/nhtool

3DNH-tool suggests a column density of $n_H \approx 4 * 10^{20}\ cm^{-2}$, which is relatively low, typical of a Galactic source. However, this value might not be reliable as it does not account for the distance of the source.

Discussion

Quasars, especially those detected in gamma rays, are usually **blazars** (AGN with relativistic jets pointed toward Earth), which can show:

- X-ray variability (on timescales of hours to days),
- Optical variability (e.g., Gaia G-band),
- Non-thermal emission across the spectrum (radio to gamma-ray),
- No strict periodicity, but sometimes quasi-periodic oscillations (QPOs) on long timescales (weeks to years).

X-ray Periodicity

X-ray Source Type	Description	Period / Periodic Behavior
Low-Mass X-ray Binaries (LMXBs)	Neutron star or black hole accreting from a low-mass star	Orbital periods: hours to a few days
High-Mass X-ray Binaries (HMXBs)	Compact object accreting from a massive OB star	Orbital periods: days to hundreds of days
Cataclysmic Variables (CVs)	White dwarf accreting from a low-mass companion	Spin periods: minutes to hours; orbital: ~80 min – 10 hrs

Magnetars / Soft Gamma Repeaters (SGRs)	Isolated neutron stars with ultra-strong magnetic fields	Spin periods: ~2–12 s; quasi-periodic bursts
Pulsars (X-ray Pulsars)	Rotating neutron stars with beamed emission	Spin periods: milliseconds to seconds
Active Galactic Nuclei (AGN)	Supermassive black holes in galaxies accreting matter	Quasi-periodic oscillations (QPOs): ~hours to days (rare)
Ultraluminous X-ray Sources (ULXs)	Extremely bright sources, possibly intermediate-mass BHs or super-Eddington accretion	Some show QPOs: ~seconds to hours
X-ray Transients	Sources with large outbursts, e.g. novae, Be/X-ray binaries	Outburst recurrence: irregular; sometimes quasi-periodic
Supernova Remnants (SNRs)	Expanding debris from stellar explosions emitting thermal X-rays	No strict periodicity; slow temporal evolution
Clusters of Galaxies	Hot intracluster medium emitting thermal X-rays	No periodicity; long-term static emission
Isolated Neutron Stars (INSs)	Cooling neutron stars; some are radio-quiet X-ray emitters	Some show spin periods: ~3–11 s
Gamma-ray Bursts (afterglows)	Transient afterglow emission observed in X-rays	Rapid decay, no strict periodicity

The instruments give different results:

- **PN:** The source exhibits a quite long period of $P = 7178.9\ s \approx 2\ h$.
- **MOS1:** No periodicity.
- **MOS2:** The source exhibits a very short period of $P = 0.718\ s$.

Only the data from the PN and MOS2 instruments observation show a periodicity. As the results differ between instruments, we chose to consider preferentially those from the instrument with the highest maximum likelihood. According to the STONKS alert document, the maximum likelihood for PN is $DetML = 66445.9$, while for M1 it is $DetML = 1016.7$ and for M2 it is $DetML = 1620.0$, supporting our decision to rely mostly on the PN data.

Discussion

The period of $7178\ s$ (approximately 2 hours) could indicate an orbital period if the source is a **compact binary** (e.g., AGN with modulation due to a companion or orbital structure), or a quasi-periodic variability linked to a jet or an accretion disk instability in the case of a **blazar**.

The fact that MOS1 detected nothing is not excluding any periodic behaviour as the value of DetML is low meaning the signal could be drown into the noise.

MOS2 detected a much shorter period which could be explained by:

- A poor temporal coverage or a too low signal to noise ratio,
- A harmonic interpretation error or aliasing,
- An analysis artifact to be verified (bias introduced by data processing or aliasing).

X-ray Spectral Properties

Xspec models

The main models that we are using are: Black body, Bremsstrahlung, Apec, Powerlaw and Gauss, or a combination of two components: Black body and Powerlaw, Bremsstrahlung and Powerlaw, Gauss and Powerlaw, and, Apec and Apec.

Black body

When an X-ray spectrum is well fitted by a black body model, it suggests that the X-ray emission is coming from a hot, dense surface or region that radiates like an ideal thermal emitter (i.e. a black body). A black body emits radiation with a spectrum that depends only on its temperature, and this emission is:

- Smooth and has a characteristic peak at a certain energy,
- Thermal, meaning it reflects a state of thermal equilibrium,
- Strongly dependent on temperature (the hotter the black body, the more it emits and the higher the peak energy).

A black body model fit generally implies that the X-rays are emitted by a compact and hot surface (not by diffuse gas). Likely sources include:

- The surface of a neutron star,
- The boundary layer in a white dwarf system (e.g., in cataclysmic variables),
- The accretion disk's inner region (if dense and hot enough),
- Or even a hot stellar photosphere.

Bremsstrahlung

When a bremsstrahlung model (also known as thermal bremsstrahlung or free-free emission) fits an X-ray spectrum well, it suggests that the X-ray emission is primarily produced by hot, ionized gas (i.e. plasma) through a specific process: Bremsstrahlung (German for "braking radiation") occurs when electrons are decelerated as they pass near atomic nuclei. This deceleration causes them to lose energy in the form of X-ray photons. This type of emission is thermal, meaning the spectrum depends on the temperature of the plasma. A good fit with this model indicates that:

- The X-ray source likely contains hot plasma.
- The X-ray spectrum is smooth and continuous, without strong emission lines (although lines may still be present if other processes are involved).

It is common in environments like:

- Accretion shocks (e.g., in cataclysmic variables, where infalling material heats up).
- Stellar coronae (like in active M-dwarfs).
- Supernova remnants or galaxy clusters.

Source of the plasma temperature: https://www.sciencedirect.com/topics/earth-and-planetary-sciences/plasma-temperature.

Astrophysical Plasma Emission Code (APEC)

When an X-ray spectrum is well fitted by an Apec model, it indicates that the emission is coming from a hot, diffuse, optically thin plasma in collisional ionization equilibrium. It models emission from a plasma that contains a mix of elements (H, He, Fe, etc.) at a certain temperature, where:

- Electrons collide with ions, exciting them,
- The ions then de-excite by emitting photons, often in the X-ray range,
- Both continuum emission (mainly bremsstrahlung) and emission lines are included in the model.

Thus, when Apec fits the spectrum, it suggests that:

- We are observing a thermal plasma (like bremsstrahlung, but with line emissions),
- The plasma is optically thin (photons escape without being absorbed),
- The plasma is in collisional ionization equilibrium, meaning the ionization state is stable and set by the temperature.

It is common in environments like:

- Stellar coronae (like in active M-dwarfs),
- Supernova remnants,
- Hot gas in galaxy clusters,
- Accretion disks or shocks in systems like cataclysmic variables (CVs),
- Flares, where gas is suddenly heated and emits thermal X-rays.

Power-law

When an X-ray spectrum is well fit by a power-law model, it means that the emission is of non-thermal origin, meaning that it doesn't come from a hot gas or a thermal surface like in blackbody or bremsstrahlung models. Instead, it points to processes involving high-energy particles, such as acceleration or scattering. Mathematically, a power-law has the form:

$$F(E) \propto E^{-\Gamma} \tag{1}$$

With $F(E)$ the flux of photon at energy E and Γ the photon index (PhoIndex in *Xspec*) typically between 1 and 3. A steeper index (higher Γ) means the spectrum drops off faster with energy.

A good power-law fit implies non-thermal emission mechanisms, such as:

- Synchrotron radiation (relativistic electrons spiralling in magnetic fields),
- Inverse Compton scattering (high-energy electrons boosting low-energy photons),
- Emission from accretion flows, like in black holes or neutron stars,
- Emission from magnetically active stars (e.g. in the tail of a flare event).

We might see a power-law spectrum from:

- Active Galactic Nuclei (AGN) because of the non-thermal emission from jets or corona,
- X-ray binaries because of the accretion-powered emission with comptonization,
- Pulsars or magnetars because of the synchrotron and curvature radiation,
- Some flare stars or M-dwarfs because of high-energy particles in flare tails,
- Cataclysmic variables (CVs) if there is a strong magnetic activity or shock jets.

Gauss

When an X-ray spectrum is well fit by a Gauss model, it means that one or more features in the spectrum, usually emission or absorption lines, are well described by a Gaussian function which is defined as:

$$f(E) = Ae^{-\frac{(E-E_0)^2}{2\sigma^2}} \quad (2)$$

Where E is the energy (in keV or eV), E_0 is the centroid energy (where the peak is), σ is the standard deviation, related to the line width and A is the amplitude, related to the line intensity.

A Gaussian profiles model spectral lines caused by atomic transitions if they are symmetric and not strongly broadened by complex physics (e.g., relativistic effects). So, if the spectrum is well fit by a Gauss model:

- There is likely a distinct emission or absorption line in the data,
- The line is symmetric and has a shape consistent with a Gaussian, suggesting relatively simple broadening mechanisms (e.g., thermal or instrumental),
- The Gaussian parameters can give physical information, such as:
    - Line center, which identifies the emitting/absorbing element or transition,
    - Line width, which gives insight into velocity dispersion, turbulence, or temperature,
    - Amplitude, which relates to the number of photons, hence the strength of the line.

Line centroid (E_0) can tell the ionization state of the emitting element. For example:

- $\sim 6.4\ keV \rightarrow$ neutral Fe (fluorescent line from reflection),
- $\sim 6.7\ keV \rightarrow$ He-like Fe ($Fe\ 55$),
- $\sim 6.97\ keV \rightarrow$ H-like Fe ($Fe\ 56$).

Line width (σ) can reveal turbulence, bulk motion, or instrumental broadening. A very broad line might hint at high-velocity material or blending of multiple unresolved lines.

Line amplitude combined with the continuum, gives info on abundances, emission measure, or plasma conditions.

In CVs for example, a $Fe\ K\alpha$ line at around $\sim 6.4\ keV$ might be modeled with a Gaussian as well as lines from other elements like O, Ne, Mg, Si. These lines are typically superimposed on the thermal continuum.

Seeing a Gaussian line in a CV spectrum might help confirm its identity. The Fe line complex is often used to distinguish magnetic CVs, especially intermediate polars, from other types of X-ray sources. Sometimes, a spectrum is fit with a thermal + one or more Gaussians to cleanly characterize both the continuum and the lines.

X-ray parameters

Here's a comparison table of the typical X-ray spectral parameters k_T (plasma temperature) and PhoIndex Γ (photon index of a power-law model) for cataclysmic variables (CVs), active stars, and active galactic nuclei (AGNs):

Source type	$k_T\ (keV)$	PhoIndex Γ	Notes
CV	- Cold component: $\sim 0.1-0.7\ keV$ - Medium component: $\sim 4-10\ keV$	Not typically used; spectra are dominated	Multi-temperature plasma models are common, especially for magnetic CVs. Spectra often include multiple thermal components and a $6.4\ keV\ F_e\ K_\alpha$ line.

	- Hot component: $\sim 16-60\ keV$	by thermal emission	
Active star	$\sim 0.1-3\ keV$	Not typically used; thermal models preferred	Emission arises from coronal plasma, often modeled with one or more thermal components. Power-law models are generally not applicable.
AGN	Not typically used; emission is non-thermal	$\sim 1.5-2.0$	X-ray spectra are dominated by non-thermal processes, modeled with a power-law. The photon index Γ typically ranges from 1.5 to 2.0.

Fit statistic

Chi-squared

The chi-squared fit statistic assumes that each bin contains enough events to approximate the Poisson distribution with a normal distribution. If some bins have under 20 counts, this test becomes unreliable. In order to be more secure, we will consider that if the bins have less than 100 counts, C-statistic should be used instead. Here, we have about 95 counts which under 100 but still close, so we will do both Chi-squared and C-statistic.

The Chi-squared χ^2 is the sum of the squared residuals, weighted by the errors in the data. The reduce Chi-squared χ^2_ν (reduced by the number of degrees of freedom) is:

$$\chi^2_\nu = \frac{\chi^2}{n_{bins} - n_{parameter}} \quad (2)$$

- $\chi^2_\nu \approx 1$: Good fit.
- $\chi^2_\nu \gg 1$: Bad fit.
- $\chi^2_\nu \ll 1$: Overfitting?

Here, the number of bins is: $n_{bins} = 51$. The number of parameters $n_{parameter}$ depends on the model:

Model	$n_{parameter}$	Main parameters
tbabs*bbody	3	nH, kT, norm
tbabs*bremss	3	nH, kT, norm
tbabs*apec	4	nH, kT, abondance, norm
tbabs*powerlaw	3	nH, PhoIndex, norm
tbabs*(bbody+powerlaw)	5	nH, kT, norm (bbody), PhoIndex, norm (powerlaw)
tbabs*(bremss+powerlaw)	5	nH, kT, norm (bremss), PhoIndex, norm (powerlaw)
tbabs*(gauss+powerlaw)	6	nH, LineE, Sigma, norm (gauss), PhoIndex, norm (pow)
tbabs*(apec+apec)	6	nH, temp1, abondance, norm1, temp2, norm2

Let's compare the most promising models (i.e. with the chi-squared closest to 1):

Criteria	Power-law	Black body + Power-law	Bremsstrahlung + Power-law
Chi-squared χ^2	40.9886	40.9886	39.2177
Reduce Chi-squared χ^2_ν (5 bins)	0.854	0.891	0.852

Column density $n_H\ (10^{22}\ cm^{-2})$	1.068e-02 ± 3.827e-03	1.068e-02 ± 3.827e-03	4.379e-03 ± 7.363e-03
$k_T\ (keV)$	X	199.358 ±-1.00	0.571 ± 0.287
PhoIndex Γ	2.813 ± 6.233e-02	2.813 ± 6.233e-02	2.716 ± 0.213
Norm	1.352e-04 ± 4.081e-06	7.378e-18 ±-1.00 (bbody), 1.352e-04 ± 4.081e-06 (pow)	1.116e-04 ± 1.333e-04 (bremss), 1.071e-04 ± 2.337e-05 (pow)
Null hypothesis probability	7.5326e-01	6.8173e-01	7.5007e-01
Degrees of freedom	48	46	46

These 3 models are fitting equivalently good, although Black body + Power-law model is slightly better.

The column density values given by the Power-law and the Black Body + Power-law models are the closest one to what 3DNH-tool suggest with $n_H \approx 10^{20}\ cm^{-2}$. The value given by the Bremss + Power-law model is around: $n_H \approx 10^{19}\ cm^{-2}$, indicating a slightly closer source which may not be coherent with an extragalactic source.

The Bremss + Power-law model's $k_T = 0.571 \pm 0.287\ keV$ is in the order of magnitude expected for a hot plasma (as in intra-galactic media or active galaxies). The k_T value of the Black Body + Power-law model is non physical suggesting that the model is not converging correctly or that the thermal component is not relevant here.

The models all yield a photon index $\Gamma \approx 2.8$, which is typical of an inverse synchrotron Compton type X-ray spectrum, compatible with a quasar detected in gamma.

The probabilities of the null hypothesis are equivalent (~ 0.7), so neither is statistically better although the Black Body + Power-law model has a slightly lower probability.

Discussion

The spectrum is very well fitted by a pure power-law model, which is typical for **quasars or blazars**, and is already suggested by Gaia DR3.

The bremsstrahlung + power-law model provides a slight improvement, but not significant enough to justify an additional thermal component with certainty. And the attempted black-body component yields an unphysical parameter, therefore discarding it.

The Apec model fits very badly which rule out active stars.

X-ray Flux and X-ray-to-Optical Flux Ratio

Optical flux

The G-band corresponds to the wavelength interval of: 330 nm to 1050 nm (https://gaia.obspm.fr/la-mission/les-resultats/article/les-observations-spectro-photometriques).

The optical flux is calculated as follow:

$$F_{optical} = F_0 * 10^{-0.4*G} \quad (3)$$

With $F_0 = 1.05 * 10^{-5}$ Gaia zero-point magnitude.

Here, we have an optical flux of $\boldsymbol{F_{optical} \approx 1.32 * 10^{-13}\ erg/cm^2/s}$.

Typical X-ray flux to optical flux ratio

The typical X-ray flux to optical flux ratio of different sources is summaries in the following table:

Object type	Typical $\frac{F_X}{F_{optical}}$ range
Active stars	< 0.1
Galaxies	$\sim 0.1 - 1$
Cataclysmic variables	$\sim 0.1 - 10$
AGNs / Quasars	> 1
Blazars / Sources Gamma	> 10

X-ray flux to optical flux ratio of our source

Chi-squared

From *Xspec* AllModels.calcFlux(".2 12.0") we obtain the X-ray flux:

- Powerlaw and Black body + Powerlaw models: $F_X \approx 7.81 * 10^{-13}\ erg/cm^2/s$,
- Bremsstrahlung + Powerlaw model: $F_X \approx 7.87 * 10^{-13}\ erg/cm^2/s$,

So, an X-ray flux of $\boldsymbol{F_X \approx 8 * 10^{-13}\ erg/cm^2/s}$ regardless of the model.

Then, we calculate the X-ray to optical flux ratio:

- Powerlaw and Black body + Powerlaw models: $\frac{F_X}{F_{optical}} \approx 5.91$.
- Bremsstrahlung model: $\frac{F_X}{F_{optical}} \approx 5.96$.

So, an X-ray to optical flux ratio of $\boldsymbol{\frac{F_X}{F_{optical}} \approx 6}$ regardless of the model.

Discussion

This value is compatible with a **quasar/AGN**, or even a low-ratio **blazar**.

Luminosity

Typical luminosity

The typical luminosity of different sources is summaries in the following table:

Object type	Typical L_X range (erg/s)
Active stars	$\sim 10^{28} - 10^{31}$
Cataclysmic variables	$\sim 10^{30} - 10^{34}$
X-ray binaries	$\sim 10^{32} - 10^{36}$
ULXs	$\sim 10^{39} - 10^{41}$
AGNs	$> 10^{42}$

Luminosity of our source

In order to calculate the luminosity L in erg/s, the source is assumed to be spherical:

$$L = 4\pi F_X d^2 \quad (4)$$

With F_X the X-ray flux calculated previously in $erg/cm^2/s$ and d the distance to the source in cm. This distance is calculated from value of the parallax given by Gaia: $P = 2.941\ mas$. We get a distance of $\boldsymbol{d \approx 1.58 * 10^{22}\ cm}$.

Chi-squared

The luminosity of the source is:

- Power-law and Black body + Power-law models: $L_X \approx 2.45 * 10^{33}\ erg/s$,
- Bremsstrahlung model: $L_X \approx 2.47 * 10^{33}\ erg/s$.

So, a luminosity of $\boldsymbol{L_X \approx 2.5 * 10^{33}\ erg/s}$ regardless of the model.

Discussion

So, with $L_X \approx 10^{33}\ erg/s$, the source does not have the luminosity expected of a typical active galactic nucleus (AGN or high-z blazar), but could correspond to:

- A weakly active quasar, if it is very distant and a weakly oriented jet is observed,
- A low-mass X-ray binary (LMXB) type variable,
- A CV (cataclysmic variable) type object or intermediate source, although the Gaia classification makes this hypothesis very unlikely.

The distance used here is $d \approx 5.11\ kpc$, based on the Gaia parallax. But if the object is an extragalactic quasar, then the Gaia parallax is false (parasitic on the luminous core). Therefore, the actual distance would be cosmological ($\sim Gpc$), which would then give a much greater luminosity, typical of AGN.

Two scenarios are possible:

1. The source is Galactic with $d \approx 5.11\ kpc$ its actual distance. The low luminosity is possible for a CV or an X-ray binary, but Gaia indicates it is a quasar.
2. The source Extragalactic (high-z quasar). Gaia parallax is probably unreliable; the true distance would be cosmological, therefore $L_X \gg 10^{33}\ erg/s$ would be coherent with a blazar.

This second scenario is the most consistent with the data set:

- Gaia: classified as a quasar with $> 99\%$ probability,
- Fermi gamma-ray detection (4FGL),
- Typical power-law spectrum of a blazar,
- Ratio $\frac{F_X}{F_{optical}} \approx 6$.

Distance

As we suppose a blazar, the distance given by Gaia DR3, from parallax measurement, is probably wrong. That is why we are going to estimate a distance from the usual blazars' X-rays luminosity which range from $\sim 10^{42}\ erg/s$ to $\sim 10^{46}\ erg/s$.

We end up with a distance of $d \approx [10^{26}, 10^{28}]\ cm$ for the source to have a luminosity corresponding to a blazar.

Documentations and Catalogues

Antonio C. Rodriguez paper

https://doi.org/10.1088/1538-3873/ad357c

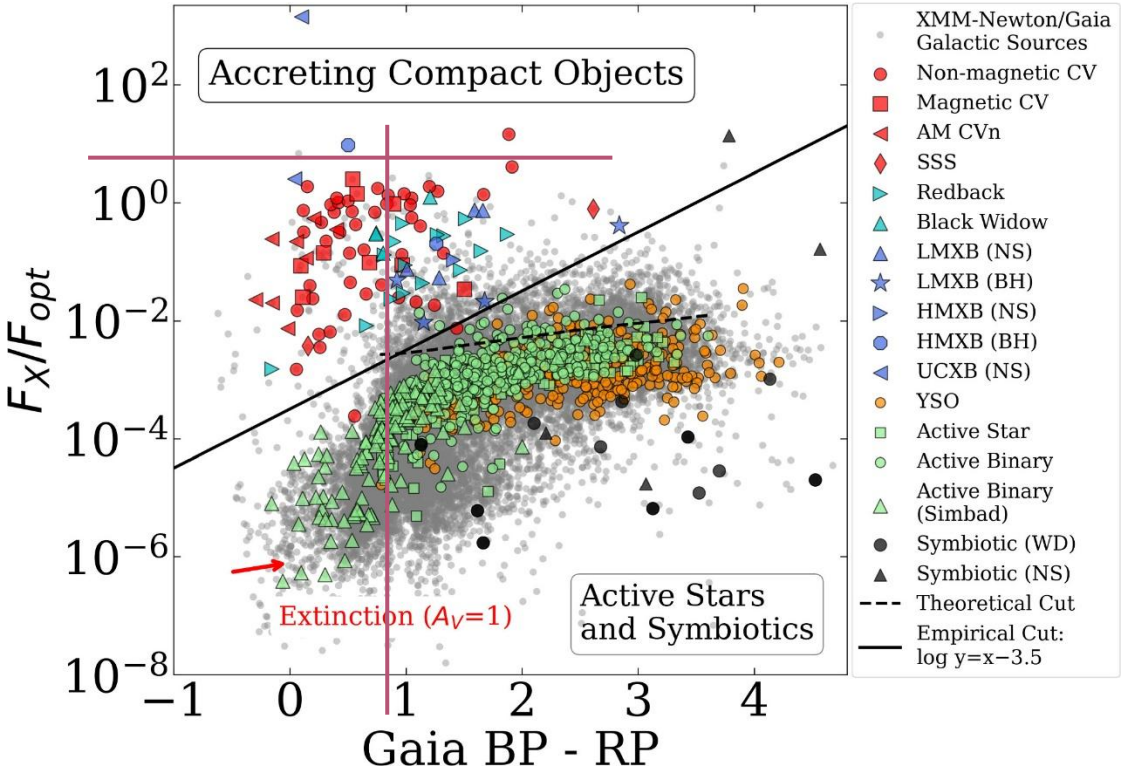

Figure 1. X-ray Main Sequence. Galactic sources from the XMM-Newton/Gaia crossmatch are shown in grey. Accreting compact object binaries in the upper left are separated from symbiotic and active stars on the bottom right by the "empirical cut" (solid line) or "theoretical cut" (dotted line). All classifications on the right-side panel are from the literature, and described in Section 2.3. No extinction correction is applied here, but the extinction vector is shown (de-reddening slides sources toward the lower left).

Gaia gives: $G_{BP} - G_{RP} = 0.8773$ and we previously calculated the ratio: $\frac{F_X}{F_{optical}} \approx 6$. Reporting these values on the figure (pink lines) our source points a lot higher than the theorical and empirical cuts indicating an **accreting compact object binary**, particularly close to a high mass X-ray binary (HMXB-BH) source. This result is totally coherent with the previous conclusions.

Tommaso Maccacaro et al. paper

https://articles.adsabs.harvard.edu/pdf/1988ApJ...326..680M

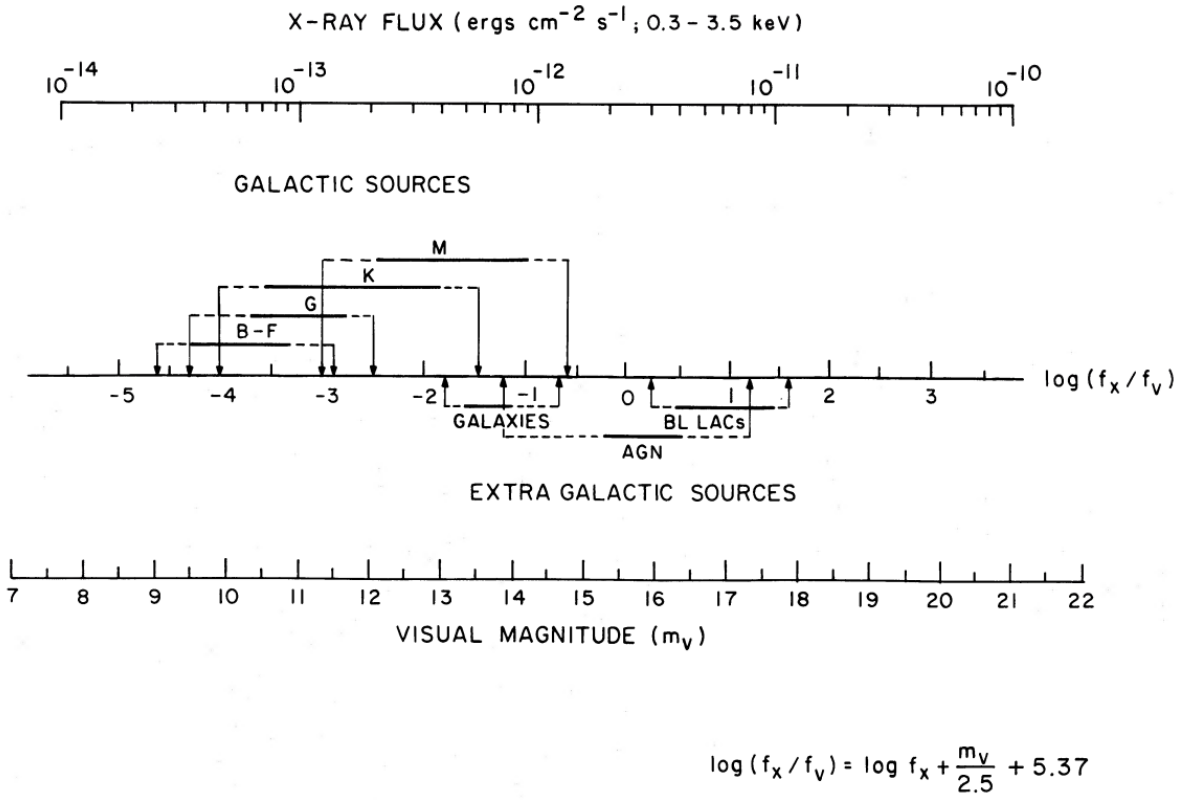

$$\log\left(f_x / f_v\right) = \log f_x + \frac{m_v}{2.5} + 5.37$$

Figure 1. Nomograph to compute the log[fx/fv], given the X-ray flux and the visual magnitude of a source. The correspondance between the various classes of X-ray sources and their typical log[fx/fv] is also indicated.

The figure presents a nomograph to compute the $\log\left(\frac{f_X}{f_v}\right)$ given the X-ray flux f_X in the $0.3 - 3.5\ keV$ band in ergs/cm^2/s and the visual magnitude m_v of the source:

$$\log\left(\frac{f_X}{f_v}\right) = \log(f_X) + \frac{m_v}{2.5} + 5.37 \qquad (5)$$

With f_v the visual flux.

For m_v we take the magnitude $G = 19.7505$ given by Gaia DR3, as previously.

Chi-squared

From *Xspec* AllModels.calcFlux(".3 3.5") we obtain the X-ray flux:

- Power-law model: $f_X \approx 5.61 * 10^{-13}\ erg/cm^2/s$.
- Bremsstrahlung + Power-law model: $f_X \approx 5.56 * 10^{-13}\ erg/cm^2/s$.

The logarithm is then:

- Power-law model: $\log\left(f_X/\mathrm{f_v}\right) \approx 1.02$.
- Bremsstrahlung + Power-law model: $\log\left(f_X/\mathrm{f_v}\right) \approx 1.02$.

So, a logarithm of $\mathbf{\log\left(f_X/f_v\right) \approx 1.02}$.

At this value, the classification as an AGN is overlapping with the BL LAC (BL Lacertae) one. But either are satisfying in regard to our precedent results.

Dacheng Lin, Natalie Webb et al. paper

https://dx.doi.org/10.1088/0004-637X/756/1/27

The Dacheng Lin, Natalie Webb et al. paper discusses multi-wavelength data using X-ray hardness ratio.

XMM-Athena Catalogue

https://xmm-ssc.irap.omp.eu/xmm2athena/catalogues/

Unclassified.

Possible Classifications

Blazar

All evidence points toward 4FGL J0333.4-2705 being a blazar, specifically a Flat-Spectrum Radio Quasar (FSRQ) or a low-synchrotron-peaked (LSP) BL Lac object, based on:

Source Identification, Counterparts and Properties

- Simbad identification as a Gamma-ray source *4FGL J0333.4-270*5 (fermi-LAT detection), with the BL possibility,
- Multiwavelength detection: EPIC Stack (Soft X-ray), XMM Slew (Soft X-ray), eROSITA eRASS1 main (Soft X-ray), XMM-SUSS 6.2 (UV to Optical), Gaia DR3 (Optical), Euclid MER Q1 (Optical to Near-IR), and AllWISE (Near-IR to Mid-IR),
- Gaia DR3 classification as a quasar with a probability of 0.9957.

Distance from parallax $P = 0.1954\ mas \rightarrow d \approx 5.11\ kpc$: uncertain for quasars. If we assume a quasar, the distance would be $d \approx [10^{26}, 10^{28}]\ cm \rightarrow d \approx [0.032, 3.2]\ Gpc$.

X-ray Variability and Periodicity

- **PN:** Period of $7178\ s$ (if true).

Low-significance variability; not robust enough to claim pulsations. Consistent with blazar or AGN light curve flickering.

X-ray Spectral Analysis

- Spectral fits consistent with power-law ($\chi^2_\nu = 0.854, \Gamma = 2.81 \pm 0.06$): strong non-thermal X-ray power-law spectrum,
- Column density: $n_H \approx 10^{22}\ cm^{-2}$, typical of low-absorption extragalactic sources,
- X-ray flux: $F_X \approx 4 * 10^{-14}\ erg/cm^2/s$,
- Null hypothesis probability: ~75%, indicating statistically acceptable fits.

Alternative model: Bremsstrahlung + Power-law (χ²_ν = 0.852), marginally better fit but not physically significant.

No evidence for significant thermal components (blackbody yields nonphysical $kT \sim 199\ keV$).

Flux and Luminosity

- X-ray to optical flux ratio: $\frac{F_X}{F_{optical}} \approx 6$, consistent with AGN/Quasar,

- Accreting compact object binary area (above the empirical cuts) of Antonio C. Rodriguez paper figure 1,
- Value $\log(f_X/f_v) \approx 1/02$, consistent with AGN and overlapping with the BL LAC.

Unrealistically low X-ray luminosity $L_X \approx 10^{33}\ erg/s$ if Gaia parallax is taken at face value, strongly supporting an extragalactic origin with a cosmological redshift.

References

Astronomical databases

XMM-Newton Science Archive (https://nxsa.esac.esa.int/nxsa-web/#search).

ESASky (https://sky.esa.int/esasky).

3DNHTOOL (http://astro.uni-tuebingen.de/nh3d/nhtool).

XMM-Athena catalogue (https://xmm-ssc.irap.omp.eu/xmm2athena/catalogues/).

Journal

ScienceDirect (https://www.sciencedirect.com/topics/earth-and-planetary-sciences/plasma-temperature).

Scientific papers

Kado-Fong, E. et al. (2016), *M Dwarf Activity in the Pan-STARRS1 Medium-Deep Survey: First Catalog and Rotation Periods*, The Astrophysical Journal, Volume 833, Issue 2, article id. 281, 19 pp. (https://ui.adsabs.harvard.edu/abs/2016ApJ...833..281K/abstract).

Antonio C. Rodriguez (2024), *From Active Stars to Black Holes: A Discovery Tool for Galactic X-Ray Sources*, PASP **136** 054201 (https://doi.org/10.1088/1538-3873/ad357c).

Tommaso Maccacaro et al. (1988), *The X-ray spectra of the extragalactic sources in the einstein extended medium sensitivity survey*, The Astrophysical Journal, 326:680-690 (https://articles.adsabs.harvard.edu/pdf/1988ApJ...326..680M).

Dacheng Lin et al. (2012), *Classification of x-ray sources in the XMM-Newton serendipitous source catalog*, ApJ **756** 27 (https://dx.doi.org/10.1088/0004-637X/756/1/27

L. Mignon et al. (2023), *Characterisation of stellar activity of M dwarfs. I. Long-timescale variability in a large sample and detection of new cycles*, A&A 675, A168 (https://doi.org/10.1051/0004-6361/202244249).

Emily K. Pass et al. (2023), *Active Stars in the Spectroscopic Survey of Mid-to-late M Dwarfs within 15 pc*, The Astronomical Journal, 166:16 (14pp) (https://iopscience.iop.org/article/10.3847/1538-3881/acd6a2).

Website

https://gaia.obspm.fr/la-mission/les-resultats/article/les-observations-spectro-photometriques